IEEE Access
Multidisciplinary | Rapid Review | Open Access Journal

Received January 10, 2020, accepted March 11, 2020, date of publication March 18, 2020, date of current version April 20, 2020.

Digital Object Identifier 10.1109/ACCESS.2020.2981661

Hybrid Optical-Radio Transmission System Link Quality: Link Budget Analysis

HASNAIN KASHIF [1], MUHAMMAD NASIR KHAN [1], AND ALI ALTALBE [2]

[1] Department of Electrical Engineering, The University of Lahore, Lahore 54000, Pakistan
[2] Faculty of Computing and Information Technology, King Abdulaziz University, Jeddah 80258, Saudi Arabia

Corresponding author: Hasnain Kashif (h.kashif13@gmail.com)

This project was funded by the Deanship of Scientific Research (DSR), King Abdulaziz University, Jeddah, under grant No. (D-85-611-1441). The authors, therefore, gratefully acknowledge DSR technical and financial support.

ABSTRACT From the last few decades' radio frequency (RF) spectrum remained attractive for wireless/wire-line applications. RF spectrum becomes dense and occupied, which makes its availability difficult to other broadband channels. Free space optical (FSO) communication, which was used for messaging/indication in the ancient days, now becomes more popular and attractive in the new era. The popularity of FSO is due to its freely available large spectrum, inherited secure links and ease of deployment. However, FSO link has to face certain challenges, e.g., line-of-sight (LOS) requirement, link attenuation due to atmospheric turbulence and severe weather conditions. To overcome the issues of FSO communication, hybrid optical-radio transmission system is proposed by which we can get maximum benefits of both spectrum. Considering the proposed transmission system link quality, link budget analysis is done in the presented work. Link budget design of transmission system is important to analyze and give recommendations.

INDEX TERMS Free space communication (FSO), link budget analysis (LBA), radio frequency (RF), signal dependent Gaussian noise (SDGN), signal independent Gaussian noise (SIGN).

I. INTRODUCTION

From the last few decades, the radio frequency (RF) communication has gained market interest because of its enormous benefits. However, there are many limitations, which impose challenges for the deployment of additional broadband channel in the existing electromagnetic spectrum [1], [2]. The crucial limitations include spectrum in-efficiency and licensing cost. Therefore, there is a dire need to have an alternative band, which supports additional broadband channels. Free space optical (FSO) communication is a promising technology, which offers huge and unregulated bandwidth with many inherited benefits. These benefits are high data rate, non-interfering nature, highly secured links and easy to install [3]–[5]. However, despite having such great benefits, FSO also suffers many drawbacks. These drawbacks are line-of-sight (LOS) requirement, limited distance and severely affected FSO link by weather (fog and snow) [5]–[7].

No doubt that FSO provides many benefits, i.e., supporting high data rate for short-range transmission, interference free links and license free bandwidth but the undesirable effects of the atmospheric turbulence induced fading, attenuation due to different weather conditions (i.e., fog, snow and smoke)and at last but not the least, the pointing errors. The pointing errors, induced due to the building sway, greatly impact on the advantages of the relay-based FSO communication system. The severe impacts of pointing errors on the system performance are evaluated rigorously in [8]. However, the proposed research work about the hybrid FSO/RF is restricted to scintillation and weather conditions for FSO link and the effect of pointing errors has been ignored. For a more realistic and pragmatic situation, it is recommended to consider the effects of pointing errors [9]. Pointing errors greatly limits the performance of FSO links mostly due to the misalignment between transmit and receive apertures and the most prominent reason is the wind, earthquake and thermal expansion. To overcome the misalignment issues, optical beams with large radius can be exploited but at the price of reduced power levels or increased error rate at the receiver and less link security. Therefore, it is claimed to perform the beam width optimization in order to achieve best error rate and geometric signal losses [9]–[11].

The reliability and connectivity of FSO link is highly weather dependent, which greatly degrades the system

The associate editor coordinating the review of this manuscript and approving it for publication was Shree Krishna Sharma.

performance [6], [7]. The reliability or robustness of a communication system can be defined as the ability to maintain certain system performances under severe channel conditions. Recently many ideas have been put forward by the research community to overcome the issues of both technologies (i.e., RF and FSO) [12]–[15]. These ideas are in the form of hybrid communication system that works differently for different systems. It was suggested to have independent links and also dependent links with different scenarios of deployment. Each system has its own merits and demerits. We have already presented research [13] with some of the above ideas and we consider independent hybrid communication system. In our previous work, we discuss about the adaptive system considering the optimization rules. The focus was to transmit maximum power through the good channel (clear weather) and minimum through the bad channel (sever weather).

Other better solution is to overcome the issues of FSO communications have been done in the literature by many researchers [16]–[23]. Authors in [17], [18] evaluate the performance of hybrid FSP/RF communication system considering the multiple RF antennas with the mmW RF channel. It is seen from [18], [19], [24] that using more than single RF antenna improves the system performance. The proposed research is to evaluate the link budget analysis by giving few practical values of different RF and FSO parameters. To further shows the better insight and understanding of the proposed research work, simulation result is presented in Fig. 6. The simulation results show the performance of hybrid FSO/RF link versus FSO only link under various weather conditions, i.e., fog and snow. It is seen from the simulation results that the hybrid link shows better performance in both foggy and snowy condition as compared to the FSO only link. The proposed work is considering the terrestrial communication system and the link is evaluated on the communication system. In the proposed research, the work is restricted to the evaluation of pragmatic parameters only and the implementation of QoS has been ignored for the current scenario. However, a preliminary discussion about the implementation of call quality has been discussed in [25]–[27].

The main goal of the proposed work is to provide link budget analysis of hybrid FSO-RF transmission system. The total received power of the system has been calculated and focuses on the challenges to the transmitted signal strength loss. The signal strength loss occurs due to different components including weather attenuation, link distance loss and atmospheric turbulence. Each component shares its own part to the main signal power loss. The link quality is very much affected due to these components. To minimize the signal losses and weather attenuation, various design approaches have been investigated [28]. Transmitter wavelength selection and link distance could be adjusted to minimize the optical signal attenuation and maximize the link quality. Analysis and simulation results are provided to support the proposed system. The contributions of the paper are highlighted below;

- To the best of our knowledge, the performance parameters in the presence of scintillation and path loss attenuation have been derived only for the FSO only link and not for the hybrid FSO/RF system. The proposed system also includes the path loss due to different weather scenarios over the FSO and RF channel.
- The performance analysis of the hybrid FSO/RF communication system has been restricted to the atmospheric turbulence induced fading for FSO link in our prior work [5], [6]. Therefore, it is essential to investigate the link budget analysis of the hybrid FSO/RF system considering the effects of scintillation and weather attenuation. The analysis has been presented to calculate the optimum parameters required for the pragmatic scenarios.
- A more simple analysis is performed for the probability density function (PDF) of Gamma-Gamma faded FSO links with the RF channel modeled as additive white Gaussian noise (AWGN). The parameters evaluation and the link budget analysis of the proposed system have been carried out by providing the simulation results.

II. OPTICAL TRANSMISSION SYSTEM

FSO is a type of unguided or wireless communications in the optical domain. In the early stage, FSO communication was developed for satellite and remote military applications. Currently, it is regarded as one of the most potent last mile and point-to-point technology. FSO communication system offers great potential for low-cost, time-constrained and high-bandwidth connectivity in many applications [6], [29]. It has the potential to accommodate additional broadband channels to meet the demands of high data rate and bandwidth hungry applications [5], [6], [30]. The other merits of the FSO communication technology include quick installation setup, license-free operation and high transmission security. However, its performance is highly susceptible to the atmospheric channel variations. Its disadvantage comparing to other wireless communication systems is the link distance which is limited up to several 10's of kilometres (km) because of atmospheric effects and it can not propagate through obstacles [29], [30].

A typical FSO communication system block diagram is shown in Fig. 1. Major components of FSO transmission system are transmitter, channel and receiver. The transmitter comprises of channel encoder (ENC), mapper (MAP), Laser/LED, lens and telescope, whereas, the receiver has PIN/APD detector, de-mapper (D-MAP) and decoder. Detailed explanation of each component is compromising and the concentration is on the main problem of link budget analysis. For LBA analysis, a brief detail is provided on different FSO link attenuating parameters before hand.

A. ATMOSPHERIC ATTENUATION

Atmospheric attenuation or climatological variation is a great design and deployment challenge for the FSO communication system. Major challenge to FSO system installation is the

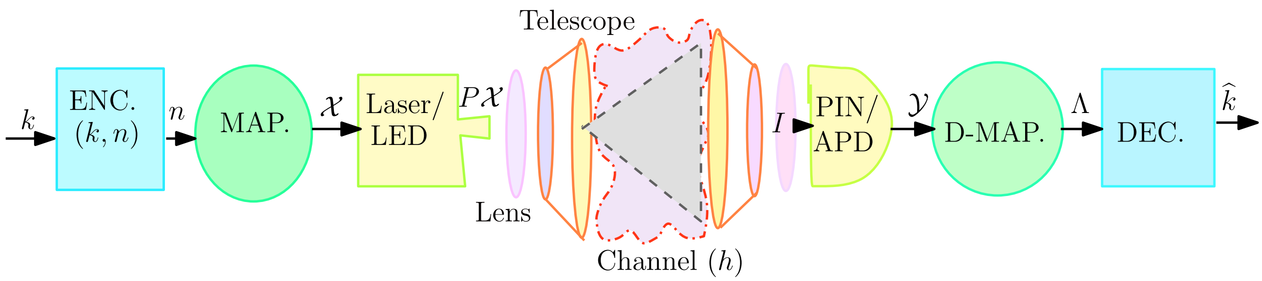

FIGURE 1. Free space optical communication system.

atmospheric attenuation caused by absorption and scattering [6]. Water particles and carbon dioxide are the main causes of absorbing optical signals whereas fog, rain, snow and clouds are the main causes of scattering optical signal in free space [6]. Atmospheric attenuation and unpredictability of weather conditions limits the communication distance and affects the link reliability [31], [32].

Fog: Atmospheric attenuation of FSO communication systems is dominated by fog, which is the most significant attenuating factor among various weather conditions. The main reason of such high attenuation in different foggy environment is that the size of fog particles is comparable to the operating wavelengths of optical waves. It is a type of cloud packets comprising of small water droplets, ice and smoke ranges from 0.1 to 50 microns in diameter [31]. Scattering results in the redistribution of the optical energy, which significantly attenuates the received optical signal intensity. Different scattering can happen depending on the size of particles such as Rayleigh, Mie and non-selective [6]. The optical attenuation is reported up to 130 dB/km under moderate conditions and 480 dB/km under dense conditions ([31] and references therein).

Fading due to fog is not well understood and difficult to characterize physically. However, an alternate approach is used to predict fog attenuation based on visibility range information. A significant path-loss occurs due to low visibility under sever weather conditions. To characterise the attenuation of optical signal propagating through the medium, specific attenuation ($\mathcal{A}(\lambda_{op})$) is used and is given by [33],

$$\mathcal{A}(\lambda_{op}) = 10 \log \left(\exp \left(\mathcal{L} \times L\right)\right) \tag{1}$$

where $\mathcal{L}$ represents the atmospheric attenuation coefficient and L represents the link distance. To predict fog attenuations based on visibility range, most widely used methods are Kruse and Kim [34]. The fog specific attenuation ($\mathcal{A}_F$) can be expressed as a function of visibility, distribution size of the scattering particle q and the operating wavelength λ_{op} [34] and is given as,

$$\mathcal{A}_F = \frac{10 \log V\%}{V} \times \left(\frac{\lambda_{op}}{\lambda_0}\right)^{-q}, \tag{2}$$

where V denotes the visibility range, $V\%$ is the transmission of air drops to percentage of clear sky and λ_0 is the visibility range reference. According to [34], q is expressed as,

$$q = \begin{cases} 1.6 & \text{if } V > 50 \text{ km} \\ 1.3 & \text{if } 6 \text{ km} < V < 50 \text{ km} \\ 0.585 V^{\frac{1}{3}} & \text{if } V < 6 \text{ km} \end{cases} \tag{3}$$

It is seen from (3) that for higher operating wavelength, the attenuation effects less severely.

Rain and snow: Rain and snow also affect the FSO propagation but the impact of these factors is not as significant as that of fog [6], [31]. The reason is that the radius of the raindrops and the size of snowflakes are significantly larger compared to the operational wavelength of the FSO light sources. The specific attenuation ($\mathcal{A}_R$) over a rainfall rate (R) for an optical communication link is given by [6],

$$\mathcal{A}_R = 1.076 R^{0.67}, \tag{4}$$

whereas, the attenuation due to snow is categorised by dry and wet snow attenuation. If S is defined as the snow rate in mm/hr, then the specific attenuation ($\mathcal{A}_S$) due to snowflakes in dB/km is given by [6],

$$\mathcal{A}_S = a S^b \tag{5}$$

where a and b are the frequency and temperature dependent constants. Rain can cause 20-30 dB/km attenuation at a rain rate of 150 mm/hr and snow can cause more than 45 dB/km [6], [33], [34]. Over the dense fog and cloud, specific attenuation is not that effective for the given wavelength, whereas better visibility, e.g., over 6 km, specific attenuation is well dependent on the operating wavelength as shown in Fig. 2. For clear sky condition, e.g., over 20 km, dependence of the attenuation on wavelength again decreases. Figure 3 shows the relationship of received power and the link distance for a given operating wavelength. It is very clear that the received power becomes weak over large distance and vice versa. While on the other hand, it is also noticed that the transmission link shows better strength over 1550 nm compared to 950 nm and 850 nm.

B. OPTICAL SCINTILLATION

In hot and dry weather, turbulence effects degrade transmission performance of the communication system. During the day, the terrain heats up more than that at night-time, causing the air nearest the ground to be more hotter than that above

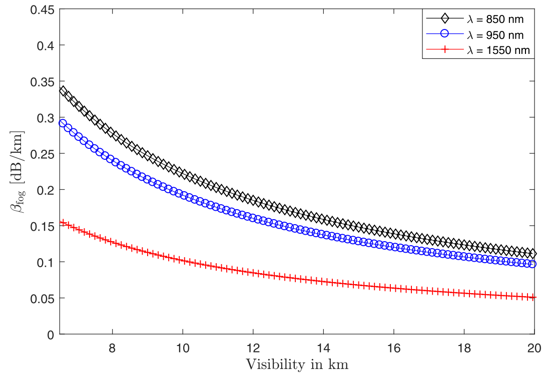

FIGURE 2. Specific attenuation over the visibility.

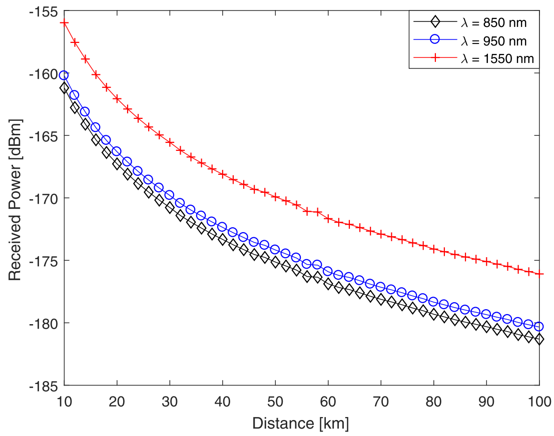

FIGURE 3. Received signal power over the varying link distance.

[5], [6]. Due to this temperature variations, some air particulates heat up more as compared to others, which changes the index of refraction. Refractive index inhomogeneities of the turbulent air causes beam spreading, beam wandering and intensity fluctuations. Also because of these inhomogeneities, the atmosphere acts like a set of small prisms and lenses that create random fluctuations in the optical beam during propagation [31], [35]. Optical scintillation is the result of these random fluctuations induced in the index of refraction [32], [35].

The optical turbulent medium which causes optical scintillation is shown in Fig. 4. In the literature [32], [35], the normalised variance of intensity known as scintillation index is used to denote the statistical characteristic of the light intensity and is expressed as [6], [13], [35],

$$\sigma_I^2 = \frac{\mathbb{E}\{I^2\}}{[\mathbb{E}\{I\}]^2} - 1, \tag{6}$$

where I denotes the received irradiance and $\mathbb{E}$ is the ensemble average operator.

Scintillation is generally classified as weak, moderate and strong. The distribution of the irradiance fluctuations is dependent on the strength of optical turbulence. According to [6], [13], [35], the scintillation distribution under weak optical turbulence has been shown to be lognormally distributed. For strong turbulence, the distribution tends to an exponential distribution [35]. Whereas, for moderate turbulence condition the theory is less well understood. Proposed distributions such as the Beckmann, Gamma-Gamma and K-distribution are based on heuristic arguments [35].

According to [36], it is found that the moderate turbulent condition is very well modeled by a lognormal distribution and its PDF is given by,

$$p^{weak}(I) = \frac{1}{\sqrt{2\pi\sigma_{\ln I}^2}I} \exp\left[-\frac{(\log(I) - \mu_{\ln I})^2}{2\sigma_{\ln I}^2}\right], \tag{7}$$

where log(.) is the natural logarithm, $\mu_{\ln I}$ and $\sigma_{\ln I}^2$ denotes the mean and variance of the logarithm of I. It is noted that for a given SI, according to [35], the distribution parameters are set as $\mu_{\ln I} = -0.5 \times \sigma_{\ln I}^2$ and $\sigma_{\ln I}^2 = \log(\sigma_I^2 + 1)$.

Similarly, for strong turbulence, the distribution tends to be an exponential distribution [6],

$$p^{strong}(I) = \frac{1}{\mu_I} \exp\left(-\frac{I}{\mu_I}\right), \tag{8}$$

where $\sigma_{\ln I}^2 \triangleq \langle(\ln I - \mu_{\ln I})^2\rangle$ represents the log-irradiance variance, $\mu_{\ln I} \triangleq \langle \ln I\rangle$ and $\mu_I \triangleq \langle I\rangle$. Whereas, for moderate turbulence condition the theory is less well understood. Proposed distributions such as the Beckmann, Gamma-Gamma

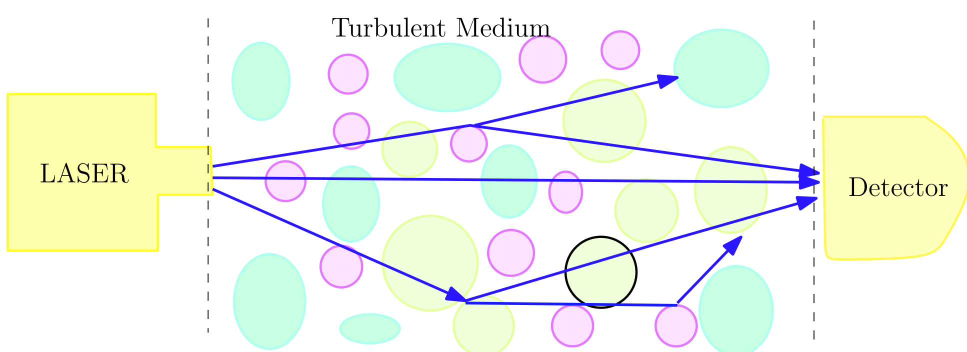

FIGURE 4. Optical turbulent medium.

and K-distribution are based on heuristic arguments. The Beckmann distribution is [6], [35],

$$p^{Beck}(I) = \frac{(1+r)\exp(-r)}{\sqrt{2\pi\sigma_z^2}} \int_0^\infty I_0 \left\{ 2\left[\frac{(1+r)rI}{z}\right]^{1/2} \right\} \times \exp\left\{ -\frac{(1+r)I}{z} - \frac{[\ln z + (1/2)\sigma_z^2]^2}{2\sigma_z^2} \right\} \frac{dz}{z^2} \quad I > 0, \quad (9)$$

where r, z and σ_z^2 are the distribution parameters and I_0 is the modified Bessel function. The Gamma-Gamma distribution is [6], [35]

$$p^{GG}(I) = \int_0^\infty p_y(I|x)p_x(x)dx = \frac{2(\alpha\beta)^{(\alpha+\beta)/2}}{\Gamma(\alpha)\Gamma(\beta)} I^{(\alpha+\beta)/2-1} K_{\alpha-\beta}(2[\alpha\beta I]^{1/2}) \quad I > 0, \quad (10)$$

where α and β are the scattering process parameters and are directly related to the weather conditions, $K_\alpha(.)$ is the modified bessel function of the second kind and order α and Γ represents the Gamma function. Expressions for calculating the parameters α and β for various propagation conditions can be found in [35]. The K-distribution is [35],

$$p^K(I) = \frac{2\alpha}{\Gamma(\alpha)} (\alpha I)^{(\alpha-1)/2} K_{\alpha-1}(2[\alpha I]^{1/2}) \quad I > 0, \alpha > 0, \quad (11)$$

C. NOISE SOURCES

Noise sources in the FSO communication are critical factors, which affect the system performance. Optical intensity from the channel is corrupted with noise and other background light sources. The internal photo detection process fluctuations or noise limits the ability of a photodetector to detect the incoming signal. In some cases when noise power is larger than signal power, it becomes hard to distinguish the signal clearly. There are two main sources of noise in the optical receivers are *shot noise* and *thermal noise*. The shot noise is associated with the photon to electron conversion process. Because each electron carries a discrete amount of charge and the flow of electrons is subjected to small random fluctuation, a noise current σ_{sh}^2 is generated which can be expressed as [35],

$$\sigma_{sh}^2 = 2e(I_P + I_D)B, \quad (12)$$

where I_P is the photo generated current through the junction, I_D is the photodetector dark current and B is the noise bandwidth.

Thermal noise is the result of internal amplifier circuitry. Thermal noise is generated independently of the received signal and can be modelled as a Gaussian distribution. This noise is dependent on the TIA circuit topology, which can be modelled as being Gaussian or non-white [6], [35]. Thermal noise is also known as the Johnson or the Nyquist noise causing by the thermal agitation of charge carriers passing through any load and is directly proportional to the absolute temperature and is given by [35],

$$i_J^2 = 4k_{BC}T_mB \times \frac{1}{R_L} \quad (13)$$

where i_J^2 denotes the Johnson noise in Amperes, k_{BC} is the Boltzmann's constant, T_m is the absolute temperature and R_L is the load resistance. However, this noise can be reduced by cooling the responsive components to a lower temperature.

There is another type of noise called background irradiations associated with the optical signal, which may cause the deleterious effects in the FSO communication system [6], [13]. In case of avalanche photodiodes (APDs), there is an additional noise figure $F(G_M)$ along with the primary source of shot noise called the *excess noise* generated by the random avalanche process. The dark current continuously flowing through the device even for no light incident on the photodetector. It arises from the electron-hole pairs thermally generated in the p-n junction of the photodiode, which depends on the semiconductor type, operating temperature and bias voltage.

The background irradiations caused from external sources which are not the part of signal itself like the ambient light sources. Background irradiations (i.e., from sun, stars and blackbody radiations) are also collected by the lens and focused onto the photodetector along with the transmitted optical field. Background irradiations of different wavelengths (i.e., other than the wavelength of transmitted optical beam) can be reduced by using optical filtering. While background irradiations of same wavelength (i.e., as the wavelength of transmitted optical beam) are considered as the additive noise field to the optical beam [35]

III. HYBRID FSO-RF SAMPLE DESIGN

A simple block diagram of the proposed hybrid FSO-RF communication system is shown in Fig. 5. It consists of two parallel channels (FSO & RF) and single encoder and decoder pair. The information message bits k are encoded by an encoder into n-bits codeword, which is then split up into two streams, i.e., n_o-bits for the optical channel and n_r-bits for the RF channel. Then each bit stream is mapped to create the respective FSO ($\mathcal{X}$) and RF ($\widehat{\mathcal{X}}$) coded symbols, which are then transmitted simultaneously on the respective channel. The RF link modulates the base-band signal to a millimeter wave (mmW) RF carrier while the FSO link employ intensity modulation/direct detection (IM/DD). The different sampling rate and coherence time of FSO and RF have been considered in our previous work eqn. (7), (8), (13) and (28) of [1] and eqn. (1) of [13]. The purpose of the proposed research work is to calculate the link budget analysis so that pragmatic parameters will be determined.

A. FSO CHANNEL MODEL

An optical beam experiences various channel effects during its propagation through the atmosphere. Air particulate matter and thermal inhomogeneities result in absorption and

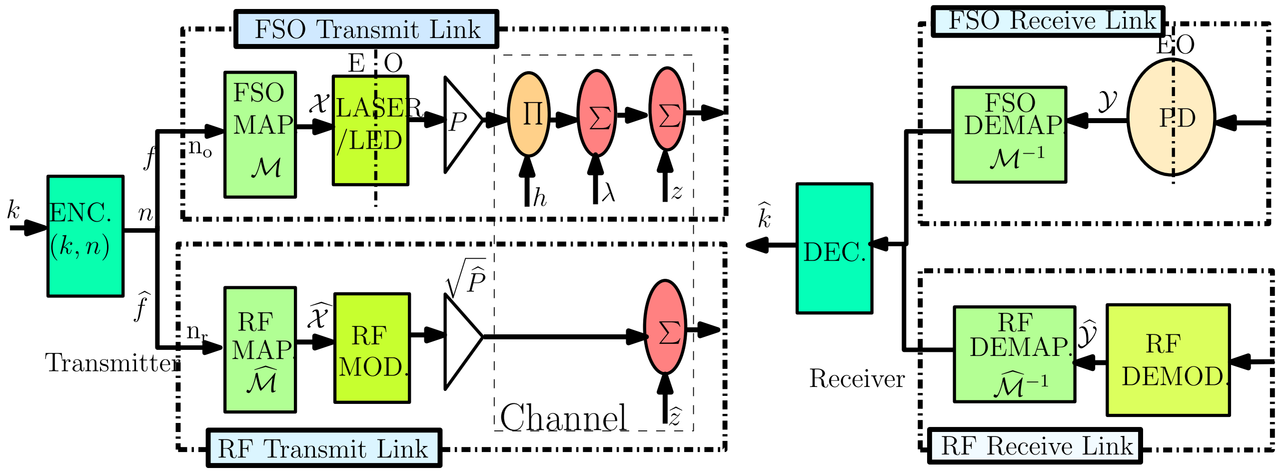

FIGURE 5. Proposed hybrid FSO/RF communication system.

scattering of the optical beam [6], [35], which causes a severe loss of optical energy. The two main ways of optical communications are non-coherent (direct detection, e.g., IM/DD) and coherent (heterodyning) [6]. In heterodyning detection system, heterodyne has to be done optically before photodetection, which makes the system more complex. Therefore, due to the design complexities of the heterodyne receiver at optical frequencies, it is preferred to use IM/DD. IM/DD is popular because of its low complexity and simple receiver design.

A mathematical model that describes the channel from the transmitter to the photodetector output for the IM/DD FSO communication system, if P be the transmit optical power on the FSO link, x is the FSO symbol transmitted using any of the defined FSO mapping schemes, then the received signal[1] assuming the signal dependent Gaussian noise (SDGN) model [1],

$$y = (\lambda + \rho gPhx) + \sqrt{(\rho gPhx + \lambda + \sigma_{th}^2)}z \tag{14}$$

where y denotes received FSO symbols, h is the FSO channel fading, λ is the background irradiation level, σ_{th}^2 is the thermal noise variance, z is the i.i.d. Gaussian random variable with zero mean and unit variance, ρ is the optical weather-dependent parameter and g represents the total FSO channel losses (i.e., antenna/aperture gains and free space loss). According to [6], we may ignore the λ contribution to the mean signal level by receiver electronics as it does not affect the input output MI of the channel. Then we can express (14) by

$$y = \rho gPhx + \sqrt{(\rho gPhx + \lambda + \sigma_{th}^2)}z \tag{15}$$

It is important to note that (14) and (15) are SDGN channels. For $\lambda + \sigma_{th}^2 \gg \rho gPhx$, the signal dependent contribution to the noise variance can be considered negligible and we can express (15) as the signal independent Gaussian noise (SIGN) model,

$$y = \rho gPhx + \sqrt{(\lambda + \sigma_{th}^2)}z \tag{16}$$

The primary factors which affect the propagating optical beam and cause transmission power attenuation and degradation of system reliability are scintillation and weather conditions such as cloud, fog, dust, haze and combinations of these [6], [31]. Although transmitter and receiver misalignment and window attenuation have certain effect on optical irradiance but in the proposed study, a line-of-sight link and perfect alignment are assumed, which is a pragmatic for most FSO applications. Therefore, the focus is on the optical scintillation and weather effects.

B. RF CHANNEL MODEL

The transmission of $\widehat{M}$-ary symbols is considered and assuming a fading free AWGN channel with RF signal power $\widehat{P}$, the received RF noisy signal $\widehat{y}$,

$$\widehat{y} = \sqrt{\widehat{\rho}\widehat{g}\widehat{h}\widehat{P}}\widehat{x} + \widehat{z} \tag{17}$$

where $\widehat{x} \in \widehat{\mathcal{X}}$ is the transmitted RF symbols after puncturing using either the BPSK or QPSK, $\widehat{z}$ is the AWGN with zero mean and unit variance.

In (20) and (21) of [13], parameters, β and $\widehat{\beta}$ are given, which are functions of the hybrid symbol period, FSO/RF total loss, RF noise spectral density and background irradiations. Therefore, the analysis involves the real link budget analysis of the FSO and RF communication system. By performing the proposed analysis, it is shown that the numerical values, which have been used in the simulation results of [13], are realistic values in terms of the link distance and FSO/RF antenna/aperture parameters. We can rewrite $\widehat{\beta}$ as,

$$\widehat{\beta} = \frac{T_{frame}}{n} \times \frac{\widehat{g}}{N_0} \tag{18}$$

[1] For the sake of simplicity, we ignore the constant scaling co-efficient (i.e., photodetector efficiency η) from the received signal model

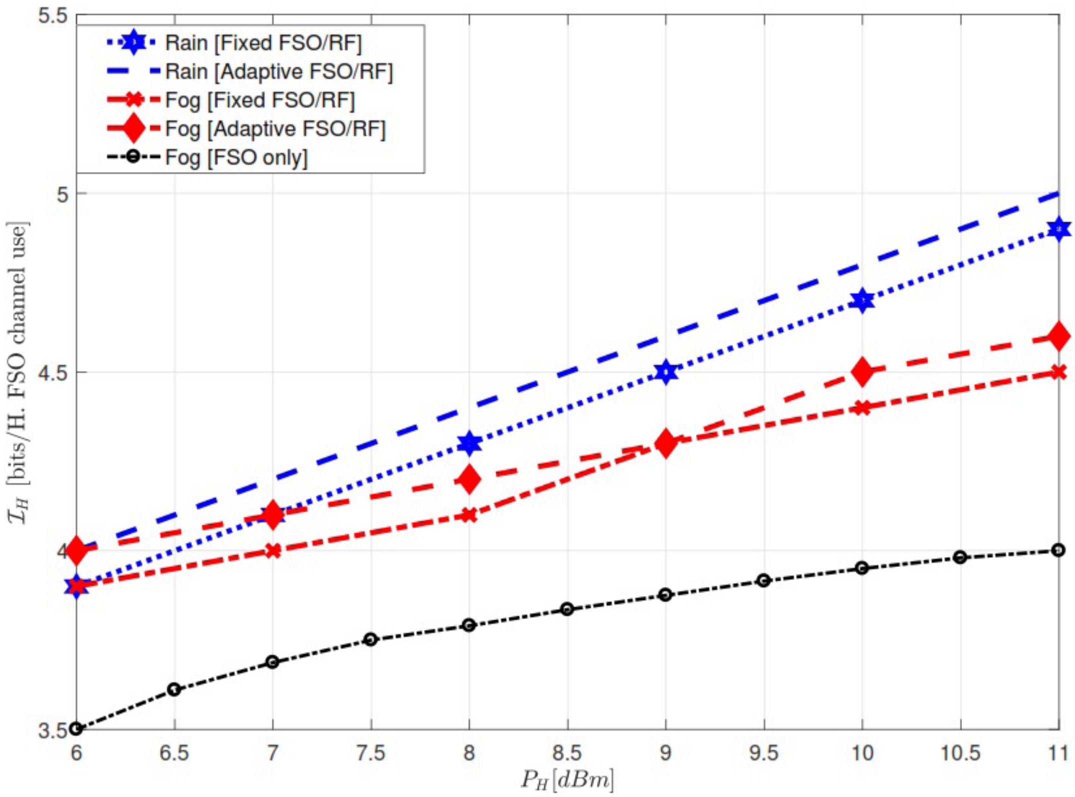

FIGURE 6. Hybrid versus fixed system for, ρ and $\widehat{\rho}$, $m = \widehat{m} = \{1, 2, 3, 4\}$ and $\beta = 30$ dB, $\widehat{\beta} = 40$dB, Rain: $\rho = 0.8$, $\widehat{\rho} = 0.3$, Fog: $\rho = 0.3$, $\widehat{\rho} = 0.8$.

where, $\frac{\widehat{g}}{N_0}$ can be estimated and then for a fixed value of $\widehat{\beta}$, $\frac{T_{frame}}{n}$ is calculated using (18). With the help of (19), $\frac{g}{\lambda}$ is calculated for a given β.

$$\frac{g}{\lambda} = \beta \times \frac{1}{\frac{T_{frame}}{n}} \tag{19}$$

Using values of $\frac{g}{\lambda}$ from (19), we can then compare its results with the practical FSO link parameters, (i.e., antenna aperture, link distance).

To evaluate both systems hybrid and FSO only, results are evaluated in different weather conditions (i.e., fog and rain) assuming the following parameters as ρ and $\widehat{\rho}$. Under the foggy condition, the weather parameters are defined to be $\rho = 0.3$ and $\widehat{\rho} = 0.8$. It can be seen from Fig. 6 evaluated using the simulation parameters given in Table 1 that the proposed adaptive system (i.e., the system optimize for the best transmission channel) gives a gain of 1 dB at $\mathcal{I}_H = 4.5$ (for the derivation of $\mathcal{I}_H$ see [13]). While in rain, the weather parameters are defined to be $\rho = 0.8$ and $\widehat{\rho} = 0.3$, it is noted from the simulation results given in Fig. 6 that a power gain of 0.5 dB at $\mathcal{I}_H = 4.5$ is obtained. It is verified that the proposed system with combined channel always gives superior performance gain under varying atmospheric conditions as compared to the FSO only link. The overall power P_H is optimally allocated to each channel of the hybrid FSO/RF transmission system under all weather conditions.

TABLE 1. Simulation parameters for hybrid FSO-RF and fixed system.

Simulation Parameters			
Parameters	**Values**	**Parameters**	**Values**
m	$\{1, 2, 3, 4\}$	$\widehat{m}$	$\{1, 2, 3, 4\}$
$beta$	30dB	$\widehat{\beta}$	40dB
Rain: ρ	0.8	**Fog**: ρ	0.3
$\widehat{\rho}$	0.3	$\widehat{\rho}$	0.8

C. RF LINK CALCULATION

Let $\widehat{g}$ as the total gain of the RF communication system, then the RF channel noise spectral density is [37],

$$N_0 = \kappa T_{sys} \tag{20}$$

where, κ is the Boltzmann's constant and T_{sys} represents the system noise temperature determined from the noise figure [37]. Using the practical parameters (i.e., link distance, antenna/aperture), the ratio $\frac{\widehat{g}}{N_0}$ can be calculated. All parameters and the corresponding calculated values are given in Table 2.

D. FSO LINK CALCULATION

Using calculated values provided in Table 2, the ratio $\frac{\widehat{g}}{N_0}$ can be calculated. Then using the values of the calculated ratio

TABLE 2. RF link parameters calculation using constant scaling factor (i.e., $\widehat{\beta}$), antenna aperture.

RF Link Budget		
Parameters	**Units**	**Values**
Transmitter Power	mW	10
Antenna Aperture	mm	400
Carrier Frequency	GHz	37
Coupling Efficiency		0.55
Link Distance	km	12
$\widehat{\beta}$		10^4
$\frac{T_f}{n}$		$8.2e^{-010}$
$\frac{g}{\lambda}$		$1.2e^{+012}$

TABLE 3. FSO link parameters calculation using constant scaling factor (i.e.,β), antenna aperture and transmit antenna beamwidth.

FSO Link Budget		
Parameters	**Units**	**Values**
Transmitter Power	mW	100
Antenna Aperture	mm	75
Wavelength	nm	1550
Coupling Efficiency		0.55
Link Distance	km	12
Transmit Antenna Beamwidth	mrad	1

in (18), $\frac{T_f}{n}$ can be evaluated for a given $\widehat{\beta}$. Using the same procedure, the ratio $\frac{g}{\lambda}$ is evaluated using (19) for a given β. The evaluation is provided in Table 3, which is calculated for particular practical parameters provided in the Table 2.

IV. HYBRID FSO-RF LINK BUDGET

For calculting the hybrid FSO-RF link budget, simple AWGN channel models are considered on both links. The AWGN FSO-RF channel parameters are calculated using the (16) and (17). The hybrid FSO-RF link budget analysis is carried out for clear sky conditions (i.e. assuming $P = \widehat{P}$, $\rho = \widehat{\rho} = 1$) and considering the binary transmission schemes. It is important to note the difference between the received signal in both the FSO and RF channel. Note that the received FSO signal is proportional to the optical power, whereas the received RF signal is proportional to the square root of the transmitted RF power. It is noted in the SNR equations (4) and (8) of both systems [13], unlike the RF system, the optical SNR depends on the square of the optical power. The ratio $\wp = \frac{\gamma}{\widehat{\gamma}}$ of SNRs of both systems can be calculated as,

$$\wp = \varrho \times \left(\frac{G_{tx}^2}{\widehat{G}_{rx}}\right) \times \left(\frac{d^2}{4\mathcal{D}\widehat{d}}\right)^2 \times \left(\frac{T_{sys}}{\widehat{T}_{sys}}\right) \tag{21}$$

whereas ϱ is the coupling efficiency, G_{tx} and $\widehat{G}_{rx}$ are the transmit and receive FSO and RF gains respectively, d and $\widehat{d}$ are the FSO and RF antenna/aperture diameters and T_{sys}, $\mathcal{D}$ denotes the propagation path length and $\widehat{T}_{sys}$ denotes the FSO and RF system noise temperature respectively. The link budget is calculated using the following practical parameters defined in Table 4. The calculation of link budget gives a certain ratio of the FSO/RF systems SNR.

It is noted from the link budget analysis in Table 4 that the difference in receive signal models influences practical parameters (i.e., FSO/RF antenna/aperture diameter and FSO transmit beam-width) required for each system. By changing

TABLE 4. Link budget is calculated based on the clear sky conditions and the ratio between the SNR is calculated as $\wp$ = [0.61, 1.93, 9.78] which depends on FSO-RF antenna/aperture diameters.

Hybrid FSO-RF Link Budget			
Parameters	**Units**	Equation	**Values**
RF Link Parameters			
Carrier Frequency	GHz	F_c	37
Link Distance	km	L	12
RF Antenna Aperture	mm	$\widehat{d}$	200
Coupling Efficiency		$\widehat{\varrho}$	0.55
RF Transmit Antenna Gain	dB	$\widehat{G}_{tx} = 10\log_{10}(\widehat{\varrho}(\frac{\pi \widehat{d}}{\lambda})^2)$	35.2
RF Receive Antenna Gain	dB	$\widehat{G}_{rx}$	35.2
Free Space Loss	dB	$\widehat{\mathcal{L}}_s = 20\log_{10}(\frac{4\pi\widehat{\mathcal{D}}}{\lambda})$	145.4
RF System Noise Temperature	K		500
FSO Link Parameters			
Wavelength	nm	λ_o	1550
FSO Transmit Antenna Beam-width	mrad	θ	0.5
FSO Receive Antenna Aperture	mm	d	150
Coupling Efficiency		ϱ	0.55
FSO Transmit Antenna Gain	dB	$G_{tx} = 10\log_{10}\left(\frac{32}{\theta}\right)^2$	69.6
FSO Receive Antenna Gain	dB	$G_{rx} = 10\log_{10}(\varrho(\frac{\pi d}{\lambda})^2)$	103.50
FSO Free Space Loss	dB	$\mathcal{L}_s = 20\log_{10}(\frac{4\pi\mathcal{D}}{\lambda})$	219.8
FSO System Noise Temperature	K		1000
Ratio Factor			
$\wp$		$d = 150$mm,$\widehat{d}$=200mm	0.61
$\wp$		$d = 200$mm,$\widehat{d}$=200mm	1.93
$\wp$		$d = 300$mm,$\widehat{d}$=200mm	9.78

the FSO receive aperture gives a large change in the respective channel SNR ratio factor. This change of ratio factor is due to the difference of proportions (i.e., $\gamma = P^2$, while $\widehat{\gamma} = \widehat{P}$) in the respective SNR of each channel model. From the link budget calculation of hybrid FSO/RF system, we can see that the system is feasible for practical applications.

V. CONCLUSION

A detailed analysis of the free space optical transmission system is provided. Major challenges to the optical link has been discussed. An alternative system was suggested. It was shown that the operating wavelength and link distance are the main contributing system parameters. It is seen that the link quality of the hybrid FSO-RF transmission system can be improved by optimizing the link distance and operating wavelength. Link budget analysis is provided in different tabulated form, which confirm the implication of the propose theoretical system with the most practical system.

ACKNOWLEDGMENT

The author would like to thank Prof. B. Cowley and K. D. Nyugen from ITR, UniSA, South Australia, for their suggestion and useful discussion during the whole journey of this research work.

REFERENCES

[1] M. N. Khan, S. O. Gilani, and M. Jamil, "Maximizing throughput of hybrid FSO-RF communication system: An algorithm," *IEEE Access*, vol. 6, pp. 30039–30048, 2018.

[2] G. R. Clark, H. A. Willebrand, and M. Achour, "Hybrid free space optical/microwave communication networks: A unique solution for ultra high-speed local loop connectivity," *Proc. SPIE*, vol. 4214, pp. 46–54, Feb. 2001.

[3] A. C. Boucouvalas, "Challenges in optical wireless communications," *Opt. Photon. News*, vol. 16, no. 9, pp. 36–39, Sep. 2005.

[4] R. M. Gagliarrdi and S. Karp, *Optical Communications*, 2nd ed. Hoboken, NJ, USA: Wiley, 2006.

[5] H. Willebrand and B. S. Ghuman, *Free Space Optics: Enabling Optical Connectivity in Today's Networks*. Indianapolis, IN, USA: SAMS Publishing, 2002.

[6] A. K. Majumdar, *Advanced Free Space Optics (FSO): A Systems Approach*, vol. 186. New York, NY, USA: Springer-Verlag, 2014.

[7] H. Tapse and D. Borah, "Hybrid optical/RF channels: Characterization and performance study using low density parity check codes," *IEEE Trans. Commun.*, vol. 57, no. 11, pp. 3288–3297, Nov. 2009.

[8] M. Usman, H.-C. Yang, and M.-S. Alouini, "Practical switching-based hybrid FSO/RF transmission and its performance analysis," *IEEE Photon. J.*, vol. 6, no. 5, pp. 1–13, Oct. 2014.

[9] W. Gappmair, "Further results on the capacity of free-space optical channels in turbulent atmosphere," *IET Commun.*, vol. 5, no. 9, pp. 1262–1267, Jun. 2011.

[10] S. Sharma, A. S. Madhukumar, and R. Swaminathan, "Effect of pointing errors on the performance of hybrid FSO/RF networks," *IEEE Access*, vol. 7, pp. 131418–131434, 2019.

[11] S. Nath, S. Sengar, S. K. Shrivastava, and S. P. Singh, "Impact of atmospheric turbulence, pointing error, and traffic pattern on the performance of cognitive hybrid FSO/RF system," *IEEE Trans. Cognit. Commun. Netw.*, vol. 5, no. 4, pp. 1194–1207, Dec. 2019.

[12] M. N. Khan, M. Jamil, and M. Hussain, "Adaptation of hybrid FSO/RF communication system using puncturing technique," *Radioengineering*, vol. 25, no. 4, pp. 644–651, Sep. 2016.

[13] M. N. Khan and M. Jamil, "Adaptive hybrid free space optical/radio frequency communication system," *Telecommun. Syst.*, vol. 65, no. 1, pp. 117–126, May 2017.

[14] G. R. Clark, H. A. Willebrand, and M. Achour, "Hybrid free-space optical/microwave communication networks: A unique solution for ultrahigh-speed local loop connectivity," *Opt. Wireless Commun. III*, vol. 4214, pp. 46–55, Feb. 2001.

[15] Z. C. Bagley, "Hybrid optical radio frequency airborne communications," *Opt. Eng.*, vol. 51, no. 5, May 2012, Art. no. 055006.

[16] M. A. Amirabadi and V. T. Vakili, "On the performance of a multi-user multi-hop hybrid FSO/RF communication system," *Opt. Commun.*, vol. 444, pp. 172–183, Apr. 2019.

[17] M. Ali Amirabadi and V. Tabataba Vakili, "Performance analysis of hybrid FSO/RF communication systems with alamouti coding or antenna selection," *J. Eng.*, vol. 2019, no. 5, pp. 3433–3437, May 2019.

[18] S. K. Shrivastava, S. Sengar, and S. P. Singh, "A new switching scheme for hybrid FSO/RF communication in the presence of strong atmospheric turbulence," *Photonic Netw. Commun.*, vol. 37, no. 1, pp. 53–62, Feb. 2019.

[19] T. Rakia, H.-C. Yang, M.-S. Alouini, and F. Gebali, "Outage analysis of practical FSO/RF hybrid system with adaptive combining," *IEEE Commun. Lett.*, vol. 19, no. 8, pp. 1366–1369, Aug. 2015.

[20] B. Makki, T. Svensson, T. Eriksson, and M. S. Alouini, "On the performance of RF-FSO links with and without hybrid ARQ," *IEEE Trans. Wireless Commun.*, vol. 15, no. 7, pp. 4928–4943, Apr. 2016.

[21] B. Makki, T. Svensson, K. Buisman, J. Perez, and M.-S. Alouini, "Wireless energy and information transmission in FSO and RF-FSO links," *IEEE Wireless Commun. Lett.*, vol. 7, no. 1, pp. 90–93, Feb. 2018.

[22] B. Makki, T. Svensson, M. Brandt-Pearce, and M. S. Alouini, "Performance analysis of RF-FSO multi-hop networks," in *Proc. IEEE Wireless Commun. Netw. Conf. (WCNC)*, Mar. 2017, pp. 1–6.

[23] B. Makki, T. Svensson, T. Eriksson, and M.-S. Alouini, "Performance analysis of ARQ-based RF-FSO links," *IEEE Commun. Lett.*, vol. 21, no. 6, pp. 1253–1256, Jun. 2017.

[24] Y. F. Al-Eryani, A. M. Salhab, S. A. Zummo, and M.-S. Alouini, "Protocol design and performance analysis of multiuser mixed RF and hybrid FSO/RF relaying with buffers," *J. Opt. Commun. Netw.*, vol. 10, no. 4, pp. 309–321, 2018.

[25] S. H. Alsamhi and N. S. Rajput, "Implementation of call admission control technique in HAP for enhanced QoS in wireless network deployment," *Telecommun. Syst.*, vol. 63, no. 2, pp. 141–151, Oct. 2016.

[26] S. H. Alsamhi and N. S. Rajput, "An efficient channel reservation technique for improved QoS for mobile communication deployment using high altitude platform," *Wireless Pers. Commun.*, vol. 91, no. 3, pp. 1095–1108, Dec. 2016.

[27] S. H. Alsamhi and N. S. Rajput, "An intelligent hand-off algorithm to enhance quality of service in high altitude platforms using neural network," *Wireless Pers. Commun.*, vol. 82, no. 4, pp. 2059–2073, Jun. 2015.

[28] H. Elayan, R. M. Shubair, J. M. Jornet, and P. Johari, "Terahertz channel model and link budget analysis for intrabody nanoscale communication," *IEEE Trans. Nanobiosci.*, vol. 16, no. 6, pp. 491–503, Sep. 2017.

[29] J. C. Juarez, A. Dwivedi, A. R. Hammons, S. D. Jones, V. Weerackody, and R. A. Nichols, "Free-space optical communications for next-generation military networks," *IEEE Commun. Mag.*, vol. 44, no. 11, pp. 46–51, Nov. 2006.

[30] A. Mansour, R. Mesleh, and M. Abaza, "New challenges in wireless and free space optical communications," *Opt. Lasers Eng.*, vol. 89, pp. 95–108, Feb. 2017.

[31] F. Nadeem, V. Kvicera, M. Awan, E. Leitgeb, S. Muhammad, and G. Kandus, "Weather effects on hybrid FSO/RF communication link," *IEEE J. Sel. Areas Commun.*, vol. 27, no. 9, pp. 1687–1697, Dec. 2009.

[32] N. Kumar and H. Sohal, "Impact of various weather condition on the performance of free space optical communication system," *J. Opt. Commun.*, vol. 35, no. 1, pp. 45–49, Jan. 2014.

[33] B. Lacaze, "Gaps of free-space optics beams with the beer-lambert law," *Appl. Opt.*, vol. 48, no. 14, pp. 2702–2706, May 2009.

[34] M. Ijaz, Z. Ghassemlooy, J. Pesek, O. Fiser, H. Le Minh, and E. Bentley, "Modeling of fog and smoke attenuation in free space optical communications link under controlled laboratory conditions," *J. Lightw. Technol.*, vol. 31, no. 11, pp. 1720–1726, Jun. 1, 2013.

[35] L. C. Andrews, R. L. Phillips, and C. Y. Hopen, *Laser Beam Scintillation With Applications*. Bellingham, WA, USA: SPIE, 2001.

[36] N. Letzepis, I. Holland, and W. Cowley, "The Gaussian free space optical MIMO channel with Q-ary pulse position modulation," *IEEE Trans. Wireless Commun.*, vol. 7, no. 5, pp. 1744–1753, May 2008.

[37] J. G. Proakis and S. Masoud, *Digital Communications*, vol. 4. New York, NY, USA: McGraw-Hill, 2001.

HASNAIN KASHIF was born in Tulamba, Khanewal, Pakistan. He received the B.S. degree in computer engineering from the COMSATS Institute of Information Technology Lahore, Pakistan, and the M.Sc. degree in electrical engineering (radio communication) from BTH Karlskrona, Sweden. He is currently pursuing the Ph.D. degree in electrical engineering from The University of Lahore (UOL), Lahore, Pakistan. He has about ten years' experience in academic field. He has worked as a Lecturer at the Department of Electrical Engineering, COMSATS University Islamabad, Lahore Campus, Pakistan. He also worked as a Visiting Faculty at Bahria University, Lahore Campus, and Bahauddin Zakariya University (BZU), Lahore Campus. He is currently working as a Faculty Member with the National College of Business Administration and Economics (NCBA&E), Lahore.

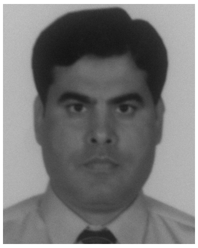

MUHAMMAD NASIR KHAN received the B.E. degree in electronic engineering from the Dawood University of Engineering and Technology, Karachi, Pakistan, in 2002, the M.Sc. degrees (Hons.) in electrical engineering one from the University of Engineering and Technology Lahore, Pakistan, and one from the Technical University of Delft, Netherlands, in 2007 and 2009, respectively, and the Ph.D. degree in telecommunications from the Institute for Telecommunication Research, University of South Australia, Australia, in 2013. He is currently working as a Professor with the Electrical Engineering Department, The University of Lahore, Pakistan. His research interests include channel coding, detection theory, development of energy efficient algorithm for wireless sensor networks, signal processing for communication, advance metering infrastructure, and optimization techniques.

ALI ALTALBE received the Ph.D. degree in information technology from The University of Queensland, Australia, and the M.Sc. degree in information technology from Flinders University, Australia. He is currently working as an Assistant Professor with the Department of IT, King Abdulaziz University, Jeddah, Saudi Arabia.